IEEE Access
Multidisciplinary | Rapid Review | Open Access Journal

Received October 16, 2021, accepted November 11, 2021, date of publication November 15, 2021,
date of current version November 23, 2021.

Digital Object Identifier 10.1109/ACCESS.2021.3128141

Applying a Dwell Time-Based 5G V2X Cell Selection Strategy in the City of Los Angeles, California

IBTIHAL AHMED ALABLANI[1,2] AND MOHAMMED AMER ARAFAH[1]

[1]Department of Computer Engineering, College of Computer and Information Sciences, King Saud University, Riyadh 11543, Saudi Arabia
[2]Department of Computer Technology, Technical College, Technical and Vocational Training Corporation, Riyadh 11472, Saudi Arabia

Corresponding author: Ibtihal Ahmed Alablani (438203904@student.ksu.edu.sa)

This work was supported by the Deanship of Scientific Research by King Saud University through Research Group under Grant RG-1440-122.

ABSTRACT The fifth generation of wireless networks is expected to provide high capacity, low latency, high reliability, and massive connectivity services. Ultra-dense network (UDN) is a clear trend for enhancing capacity, coverage, and load balancing. In UDNs, the cell selection issue for moving vehicles should be addressed. In this paper, a cell selection strategy known as a dwell time estimation (DTE) scheme is proposed, which is based on Vehicle-to-Everything (V2X) communications. It selects small cells that have the longest dwell time in a vehicle's direction to decrease handover (HO) rate. The proposed DTE scheme is evaluated using two datasets, which are 5G small cells and vehicles datasets, that were collected in the city of Los Angeles in California. The simulation result shows that our DTE algorithm outperforms other recent related schemes in terms of the mean number of HOs by up to 36.26% because it prolongs the dwell time of the vehicle within the serving small cell. Consequently, it reduces the average number of HO failures and unnecessary HOs. In addition, it gives improvements in terms of the average achievable downlink throughput and network energy efficiency. Furthermore, it has superiority over the other schemes in terms of the mean packet delay by up to 16.49%.

INDEX TERMS Los Angeles, 5G, small cells, UDNs, cell selection, dwell time, handover, V2X.

I. INTRODUCTION

Wireless cellular networks of fifth-generation (5G) technology will soon be more widely used [1]. 5G technology will bring new service capabilities for future smart cities, the Internet of Things (IoT), and vehicle applications [2], [3]. The requirements of these services are high data rate, low latency, and a massive number of connections. The ubiquity of networks across the world becomes one of the most important issues, even in challenging cases such as user mobility and high density or populated areas [4]. Vehicular communications need reliable and fast wireless connections, and Vehicle-to-Everything (V2X) systems become essential to decrease driving time and the number of accidents [5]. The term Vehicle-to-Everything (V2X) includes Vehicle-to-Network (V2N), Vehicle-to-Vehicle (V2V), and Vehicle-to-Pedestrians (V2P) [6]. 5G technology will support the requirements of future V2X applications [7].

The main features of 5G enabling technologies are massive multiple-input, multiple-output (mMIMO), Software-Defined Networking (SDN), Network Function Virtualization (NFV), Centralized Radio Access Network (C-RAN), local offloading, and small cells [8], [9]. Small cell is an umbrella term for a radio access node that has low power and a short-range [10]. 5G's small cell is a key technology that is deployed to improve network coverage and capacity and balance the traffic load among cells. They operate at high frequencies and their range is between 10 m and 2 km [11]. Millimeter-wave (mmWave) communication will play a significant role in 5G small cells [12]. The term mmWave refers to electromagnetic waves that have a short, millimeter-level wavelength, which ranges between 10 and 1 mm, and a high frequency between 30 and 300 GHz [13]. Network densification refers to deployment of dense, small-cell networks within a geographical area [14]. It is a promising

The associate editor coordinating the review of this manuscript and approving it for publication was Jie Gao.

technique that enhances throughput, spectral efficiency and connectivity [15]. Densification deployment of small cells is emerging in 5G cellular networks, resulting in ultra-dense networks (UDNs) that have interesting effects [16]–[18]. Cell selection is the process of assigning user equipment (UE) to a serving base station (BS) based on a specific criterion [19]. This process is also called user association or BS assignment [20]. In UDNs, cell selection is a critical issue that should be addressed to avoid frequent handovers (HOs) [21]. The handover process is classified based on network heterogeneity into vertical and horizontal handover [22], as shown in figure 1. A vertical handover occurs between two cells that have different network technologies (heterogeneous cells), while a horizontal handover takes place between cells that have the same type of network technology (homogeneous cells) [23]. The handover process is also classified based on the connection mechanism into hard and soft handover. A hard HO depends on the principle of break-before-make, while a soft HO is based on the concept of make-before-break [24].

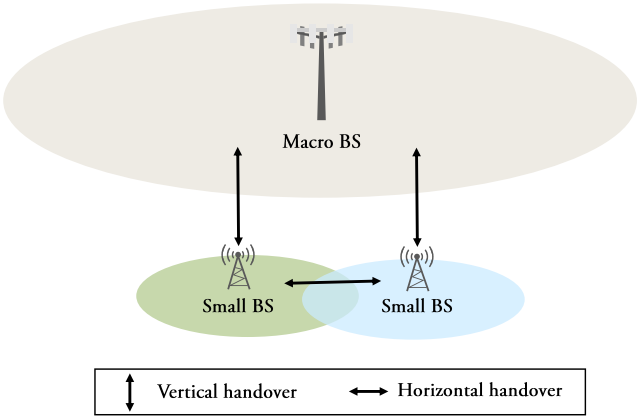

FIGURE 1. Vertical vs horizontal handovers.

The conventional cell selection method involves measuring radio-specific parameters, such as the Received Signal Strength Indicator (RSSI) and then choosing the strongest BS [25]. However, applying the conventional approach in 5G networks is not appropriate owing to the dense deployment of small cells [24], [26], [27]; considering only one factor, the RSSI, could cause unnecessary handovers, service interruptions, and unbalanced load distribution [24], [28].

In 2018, the deployment of small BSs in the United States (US) increased by 550%. The number of small BSs (SBSs) in the US is expected to exceed 800,000 by 2026 [29], [30]. The city of Los Angeles (LA) is the second-largest city in the United States by population [31]. It is located in California and has about 4 million people [32]. Based on [33], [34], there are approximately 1,796 small cells distributed throughout the city of LA. Figure 2 shows the locations of these small cells, which have three primary clusters; namely, Burbank, Central, and Long Beach. As illustrated in the figure, the Central cluster has a high density of small cells.

Most existing cell selection strategies focus on enhancing network throughput by giving high priority to the nearest small cells that have the highest RSSI values. However, rRelying on a nearby station in UDNs will increase the HO rate and have a ping-pong effect that affects the network performance; the ping-pong phenomenon refers to frequent unnecessary HOs that occur when a mobile device moves among small cells [35]. The main factor for decreasing the HO rate in UDNs is the dwell time. Dwell time is the duration spent by a user's equipment in a wireless cell. Increasing the length of dwell time will reduce the mean number of HOs and therefore diminish the probability of unnecessary HOs and HO failures.

The significance of our work and contributions comes from proposing a cell selection algorithm that maximizes the dwell time in a wireless cell to decrease the HO rate and thus enhance the achievable data rate, average energy efficiency, and DL packet delay. Also, the dwell time of a vehicle in the cell is accurately estimated based on the current location of the vehicle. Furthermore, the proposed DTE strategy has been applied in a real-world environment, based on the locations of existing 5G small cells in the city of Los Angeles, with vehicles' positions and other related information taken from real data collected in LA.

The rest of this paper is organized as follows: Section II provides a review of related works and the contributions of the paper. The proposed DTE scheme and system model are described in detail in Sections III and IV, respectively. Section V presents the simulation results for the proposed cell selection algorithm in LA city. The paper is concluded in Section VI. Appendix A represents a proof of the dwell time law, while Appendix B gives a list of all abbreviations used.

II. RELATED WORK AND CONTRIBUTIONS

A. RELATED WORK

In this section, some recent related cell selection methods that are proposed for 5G UDNs are discussed in terms of the network model, performance metrics, and evaluation results.

Tesema *et al.*, in [36], presented a novel multi-connectivity cell selection method for 5G UDNs, which uses a rapid selection of serving cells from an Active Set (AS). The proposed method applies multi-connectivity to provide ultra-reliable communication and to avoid service interruption, based on Coordinated Multi-Point (CoMP) transmission. The best cells are chosen based on the received signal power and corresponding noise power. The network was modeled as a hexagonal layout with 59 cells. In each cell, there are five UEs. The Intersite Distance (ISD) between BSs is 100 meters. A mix of slow and fast UEs is expected. The simulation results show that the proposed scheme solves the problem of connection failures owing to Radio Link Failures (RLFs). In addition, the throughput that is obtained at the 5% point of the cumulative distribution function (CDF) curve, which

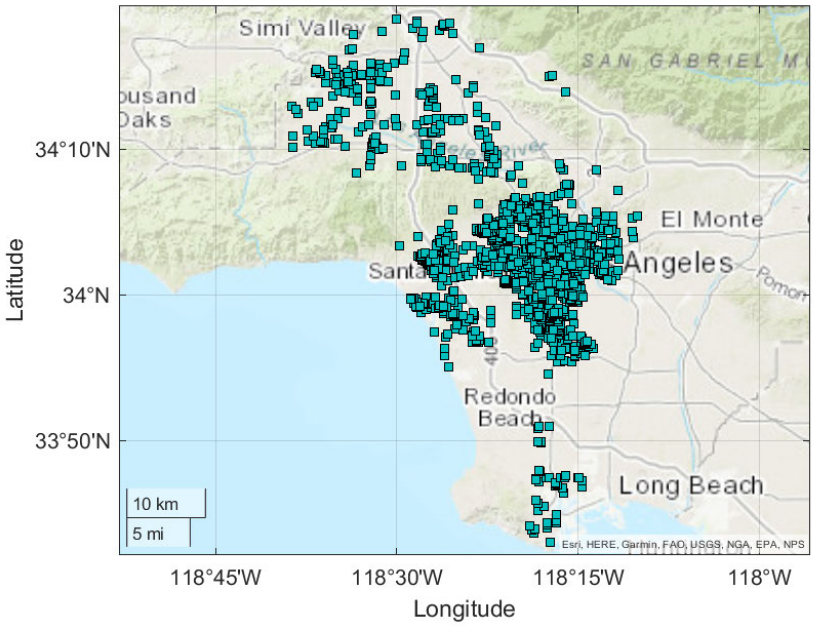

FIGURE 2. Distribution of 5G small cells throughout the city of Los Angeles.

is known as fifth-percentile throughput, is slightly improved compared to the benchmark single-connectivity solution.

Kapoor *et al.* developed four base station selection approaches that consider vehicle mobility for ultra-dense small cell urban networks in [37]. The proposed approaches are (1) minimum distance in the vehicle direction (MD-VD), (2) minimum load in the vehicle direction (ML-VD), (3) next neighbor on the same street (NN-S), and (4) next neighbor on the opposite street (NN-O). They follow three steps to select the cell to be associated with. The first step is selecting K-nearest BSs, which are called shortlisted BSs. The second step is selecting BSs from shortlisted BSs that are in the vehicle direction (i.e., BSs located in range from 0 to π). The third step varies according to the objectives of the proposed approaches. In MD-VD, a BS which has the minimum distance in the vehicle direction will be selected, while in ML-VD, the BS with the minimum load in the direction of vehicle travel will be chosen. In NN-S, the selected base station is the one that has the maximum angle in the range between 0 and $\pi/2$. In NN-O, the BS that has the minimum angle in the range between $\pi/2$ to π will be selected as a serving BS. Simulation results demonstrate that the MD-VD scheme is the least efficient of these methods in terms of HO rate.

Naderializadeh *et al.* developed a parallel dynamic cell selection (DCS) algorithm in [38]. Also, an interference management scheme is proposed to solve the problem of interference in UDNs. The downlink (DL) scenario of a cellular UDN that consists of N transmission points (TPs) and K UEs was considered. Within 200 by 200 meters^2, TPs and UEs are uniformly distributed at random. The received signal-to-interference-plus-noise ratio (SINR) and UE priority, such as proportional fairness (PF), are used to determine the UE association process. The proposed DCS algorithm has four main steps: UE-TP association, UE priorities, UE scheduling, and link scheduling. In the UE-TP association step, UEs are associated with the transmission point that has the highest SINR value. The users are ordered based on their priority in the second step, i.e., UE priorities. The serving transmission point can operate in single-user mode or multiple-users mode. The UE scheduling operation is utilized in the multiple-users mode. To enhance the effect of the interference, the decision is made to activate/deactivate selected TPs in the link scheduling step. The simulation results show that the proposed DCS scheme outperforms some benchmark methods in terms of sum-rate and network coverage.

In [39], Liu *et al.* presented a fuzzy technique for an algorithm based on the Order Preference by Similarity to Ideal Solution (TOPSIS) for 5G UDNs. The optimal neighboring cell is selected based on multiple criteria: reference signal receiving power (RSRP), SINR, and network jitter. It combines the strengths of both TOPSIS and fuzzy logic. Also, by using historical data, a subtracting clustering scheme is used to define the optimal fuzzy membership function. Sixteen BSs are deployed in a square area of 1000 by 1000 meters^2, and fourteen UEs are moved at random. The distance between each two BSs is 400 meters. The performance results show that the proposed algorithm outperforms the conventional approach in terms of the number of HOs and instances of ping-pong HO. Furthermore, Quality of Service (QoS) is maintained at a high level.

In [40], Khodmi *et al.* developed a joint user association and power allocation scheme using a non-cooperative game theory. The proposed scheme depends on the values of the downlink data rate and allocated power for the access link. It is designed for heterogeneous UDNs (HUDNs) and it aims to enhance the QoS and to balance the throughput. The game includes two sub-games, which are the backhaul game (BG) and the access game (AG). In the BG, leaders estimate the optimal power allocation schemes for their followers. The followers select the best responses to their leaders in the AG. The HUDN is modeled as a single macro BS with multiple relay nodes. UEs are randomly distributed in the cell. Compared to existing methods, the simulation results show that the proposed scheme enhances network performance in terms of throughput and UE rate. Furthermore, the optimal downlink power allocation is achieved.

Nguyen *et al.* proposed a joint user association and power allocation algorithm in [41]. It is designed for millimeter-Wave (mmWave) UDNs. A scheme called alternating descent was proposed to divide the optimization problem into two sub-problems to handle the joint problem easily. The two sub-problems are the SBS-UE association problem and the energy efficiency optimization problem. The UE association optimization problem is based on the achievable data rate, and the throughput fairness issue among users is considered, targeting the maximization of the minimum achievable data rate. The network model consists of a set of M small BSs and K UEs that are randomly distributed. The numerical results show that the proposed scheme has convergence and low complexity.

Zhang *et al.* presented a deep-learning-based user association strategy for HUDN in [42]. The user association issue is mapped into an image segmentation problem based on pixel-scale classification. A U-Net convolutional network model is constructed to perform the cell selection task under load balancing and UE fairness constraints. The input to the proposed U-Net model is the channel gain matrix, where path loss, shadowing and antenna gain are considered. The output of the trained model is the BS association matrix. The network is modeled as a two-tier HUDN that is composed of two macro BSs and eight small BSs. The BSs are distributed at random in an area of 600 by 600 meters. In terms of computation time and robustness to network scales, the simulation results show that the UDN-based deep learning method outperforms the asymptotically optimum genetic algorithm (GA) scheme.

In [43], Sun *et al.* proposed two schemes to enhance the process in HUDNs, which are based on coordinated multipoint (CoMP) technology. These schemes are known as movement-aware CoMP handover (MACH) and improved MACH (iMACH). The cell selection criterion of the MACH scheme is dwell time, while the iMACH scheme depends on both the dwell time and the closest distance. The MACH scheme passes through two steps to select n cooperation BSs. The first step is selecting the candidate BSs that have dwell times larger than a predefined threshold. The second step is selecting the cooperating BSs, which are the n cooperating BSs that have the largest RSSI values. The iMACH scheme has three steps. The first step is selecting the nearest BS and the second step is selecting the candidate BSs, which are the BSs, other than the nearest BS, that have dwell times larger than a predefined threshold. The third step is selecting the cooperating BSs which are the nearest BS and the $n-1$ cooperating BSs that have the largest RSSI values. The network is modeled as a two-tier architecture with macro and small BSs that are set based on Poisson point processes (PPP). The simulation result shows that the MACH and iMACH algorithms outperform existing cell selection schemes in terms of throughput, HO rate, and coverage probability.

In [44], Qin *et al.* proposed a HO scheme for 5G UDNs, namely, handover based on residence time prediction (HO RTP). The cell selection process is based on the values of RSSI and the predicted residence time. The small BS that has the strongest RSSI with residence duration that exceeds a predefined threshold is selected. The network is modeled as a set of small BSs that are located on the basis of Tyson's polygon distribution. In terms of average user throughput, the simulation results show that the HO RTP scheme outperforms the conventional method.

In [24], Alablani and Arafah proposed an adaptive cell selection scheme, called ADA-CS, that was designed for heterogeneous UDNs. It can adapt to different features of heterogeneous UDNs and vehicle movements. It passes through six phases to select the best BS to associate with. These phases are configuration, decision-making, filtering, narrowing, selecting, and HO triggering. The network is modeled as a hexagonal grid that has two tiers of BSs, with seven macro cells and a density of 600 small BSs per km^2. Simulation results show that the proposed ADA-CS scheme outperforms the traditional RSSI-based scheme in terms of average number of HOs by 42.39%. Moreover, it achieves superiority over related recent cell selection schemes by up to 36.53%. In addition, the ADA-CS improves the average achievable downlink data rates and spectral efficiency by up to 3.98% compared with other schemes.

Table 1 shows a comparison of recent related cell selection schemes in terms of cell selection factors and system models. Analysing the recent works represented in this section, we found the following limitations:

- Recent work focuses on enhancing the network throughput by giving a high priority to BSs that have the strongest RSSI, but at the expense of the HO rate. Owing to the frequent link switching caused by the ping-pong effect, an increase in HOs leads to packet loss [45]. Therefore, the effective achievable data rate will be reduced.
- Some studies relied on calculating the dwell time of a UE in a wireless cell but did not give it a high priority in the selection. Also, the dwell time is not accurately estimated when the UE is assumed to be at the edge of the cell, which is unsuitable for UDNs.
- Recent studies modeled UDNs as a small, non-real-world environment, such as a hexagonal grid, random,

TABLE 1. A comparison among recent related cell selection schemes.

Ref	Year	Authors	Designed for	Cell selection factors	System model
[36]	2016	Tesema et al.	UDNs	RSRP, noise power	Hexagonal grid
[37]	2017	Kapoor et al.	UDNs	Distance, vehicle direction, cell load, azimuth	Deterministic distribution
[38]	2018	Naderializadeh et al.	UDNs	SINR, UE priority (PF)	Uniform random distribution
[39]	2019	Liu et al.	UDNs	RSRP, SINR, Jitter	Deterministic distribution
[40]	2019	Khodmi et al.	HUDNs	Downlink rate, power allocation	Deterministic distribution
[41]	2020	Nguyen et al.	UDNs	Achievable data rate	Random distribution
[42]	2020	Zhang et al.	HUDNs	Channel gain, cell load, UEs fairness	Random distribution
[43]	2021	Sun et al.	HUDNs	Dwell time, distance	PPP distribution
[44]	2021	Qin et al.	UDNs	RSSI, residence time	Tyson polygon distribution
[24]	2021	Alablani and Arafah	HUDNs	RSSI, speed, azimuth, load, and cone angle	Hexagonal grid

deterministic, PPP, or Tyson polygon distribution. Furthermore, the UE is placed and moved based on non-realistic mobility information.

B. CONTRIBUTIONS OF THE PAPER

In this paper, the major contributions are as follows:

1) Proposing an effective cell selection algorithm for 5G UDNs, called a dwell time estimation DTE) scheme, which selects the small BS that has the longest dwell time. The performance of 5G networks is evaluated in terms of mean (a) dwell time, (b) number of horizontal HOs, (c) achievable downlink vehicle throughput, (d) number of horizontal HO failures and unnecessary HOs, (e) network energy efficiency, (f) packet delay. Our proposed strategy is compared with recent HO schemes called handover based on residence time prediction (HO RTP), minimum distance in the vehicle direction (MD-VD), minimum load in the vehicle direction (ML-VD), next neighbor on the same street (NN-S), and next neighbor on the opposite street (NN-O).
2) Constructing a UDN model that consists of a high density of 5G small cells. The system model is based on the distribution of small cells in the city of Los Angeles in California. In addition, vehicles are modeled based on a real dataset that was collected in LA and includes their locations and other related information.

III. THE PROPOSED DTE SCHEME

A. PROBLEM FORMULATION AND RESTRICTIONS

A This study relates to Vehicle-to-Network (V2N) communications, where vehicles are associated with the best small BS based on our proposed DTE scheme. We optimize the horizontal HO process between homogeneous small cells in 5G UDNs to prolong the dwell time of vehicles within the serving small cell. All small BSs are represented by $\mathbb{S}_{\mathbb{BS}} = \{S_1, S_2, \ldots, S_N\}$. Moving vehicles are denoted by $\mathbb{V} = \{V_1, V_2, \ldots, V_M\}$. $\mathbb{X} = \{X_{11}, X_{12}, \ldots, X_{NM}\}$ is the association vector of the UDN, where X_{nm} is the variable of association between vehicle V_m and small BS S_n. Equation (1) shows the formula of X_{nm}, which has two possible values, 1 and 0. A hard handover is considered in this work, where the connection between a vehicle and the current small cell is broken before connecting to the next small cell to save network resources and to reduce the connection complexity. A vehicle can only be connected to one small BS at a time, as given in equation (2)).

$$X_{nm} = \begin{cases} 1 & 1 \; if \; V_m \; associates \; with \; S_n \\ 0 & otherwise \end{cases} \tag{1}$$

$$\mathcal{R} : \sum_{n} X_{nm} = 1, \quad \forall \, V_m \in \mathbb{V}. \tag{2}$$

B. PROCEDURES OF THE DTE ALGORITHM

We propose a DTE strategy for UDNs that selects the BS with the longest dwell time, to reduce the HO rate. It passes through four steps to achieve its target (Figure 3). These steps are:

- **Step 1: (BSs Exploration)** Suppose that the small BSs are denoted as $\mathbb{S}_{\mathbb{BS}}$: a vehicle explores small BSs that have acceptable received signal strength based on a predefined threshold, which is represented by $\mathbb{B}'$ (equation (3)).

$$\mathbb{B}' = \{S_n | S_n \in \mathbb{S}_{\mathbb{BS}} \; \& \; RSSI_{nm} > \hat{\text{Th}}\}, \quad \forall \, V_m \in \mathbb{V}. \tag{3}$$

- **Step 2: (Dwell Time Estimation)** The dwell time in a small cell is estimated based on vehicle speed (v), the distance between the vehicle and small BS (d), and the angle between the vehicle direction and small BS (Ω). The cell dwell time is calculated by dividing the length of staying distance (L) within a small cell by the speed of the vehicle. Equation (4) represents the formula of L.

$$L = d \; cos(\Omega) + \sqrt{R^2 - d^2 \; sin^2(\Omega)} \tag{4}$$

The formula of dwell time, which is represented by T_d is shown in equation (5).

$$T_d = L/v \tag{5}$$

Proof: Please see Appendix A.

Therefore, the proposed DTE protocol is characterized by its ability to deal with changes in the features of:

- Small cells in terms of their size and geographical location.
- Vehicles in terms of their geographical location, driving speed and direction.

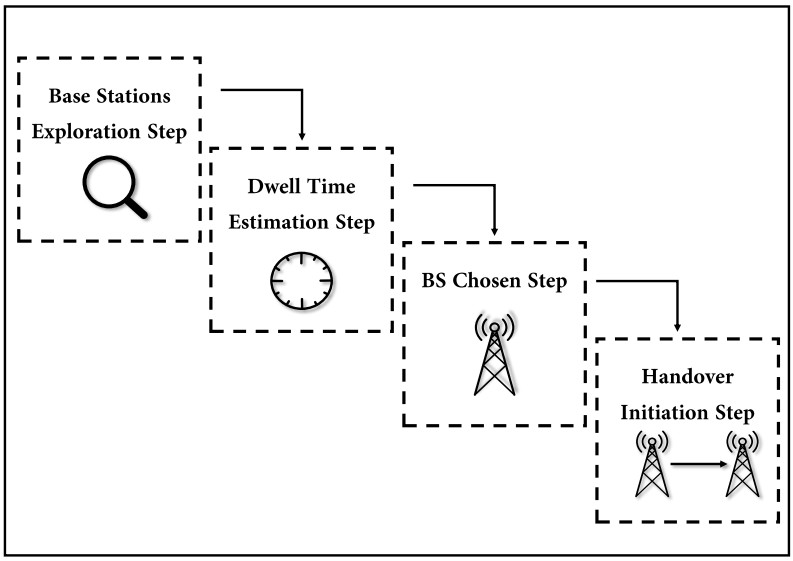

FIGURE 3. The steps of the proposed DTE scheme.

- **Step 3: (BS Chosen)** The small BS that has the longest dwell time will be selected (equation (6)).

$$\mathbb{B} = \{S_n | S_n \in \mathbb{B}' \ \& \ S_n \ has \ max(T_d)\} \tag{6}$$

- **Step 4: (HO Initiation)** The HO is initiated when the received signal strength falls below a predefined threshold, as shown in equation (7).

$$RSSI_{nm} < \hat{\text{Th}} \quad \forall \ V_m \in \mathbb{V} \ \& \ \forall \ S_n \in \mathbb{S}_{\mathbb{BS}}. \tag{7}$$

Algorithm 1: Pseudocode for the Proposed DTE Method

```
==========================================
input  : S_BS.
output: B.
/* Step 1: BSs Exploration */
Calculate B' according to (3);

/* Step 2: Dwell Time Estimation */
Estimate L according to (4);
Calculate T_d according to (5);

/* Step 3: BS Chosen*/
Calculate B according to (6);

/* Step 4: HO Initiation */
if condition (7) satisfied Then
  | Initiate HO to B;
end if
==========================================
```

C. A CASE STUDY OF THE CELL SELECTION PROCESS

In this section, a case study of the cell selection process is taken to clearly show readers how the proposed DTE approach performs the cell selection task. In addition, we explain what makes the proposed approach outperform other recent related schemes.

Let us take an example that is shown in figure 5. In this example, a blue vehicle is moving in the street and there are many small BSs distributed around it, which are represented by green squares. Suppose the diameter of the small cell is 600 meters. If the vehicle follows the HO RTP method, it selects the small BS that has the strongest signal strength with dwell time higher than a predefined threshold (e.g., 2 sec). Based on the MD-VD scheme, the small BS that has the minimum distance in the vehicle direction will be selected as a serving cell. We find that the HO RTP and MD-VD schemes choose the same small BS because they depend on the same principle, which is to give priority to the nearest cell. If the NN-S scheme is applied, the small base station located in the right quarter of the vehicle with the minimum angle will be chosen. When the NN-O scheme is considered, the small BS that is on the left quarter of the vehicle with the minimum angle will be selected. The chosen cell is farther from the cells that are selected according to the previous methods and it has a longer dwell time for the vehicle within it. Based on our DTE scheme, the selected small BS is the BS in which the vehicle can receive its signal and has the longest dwell time, based on equation (35) that has been proven in appendix A. We gave a high priority to the staying time of the vehicle within the small cell because this will:

- Minimize the number of horizontal HO: There is an inverse relationship between the dwell time and the number of HOs; the longer the cell's dwell time, the fewer the number of HOs.
- Enhance the average achievable data rate and energy efficiency: When the vehicle moves forward, it will reach the middle of the serving cell and will achieve a high data rate that other methods may not be able to achieve. Therefore, the average achievable data rate will be higher than in the other methods. In addition, the

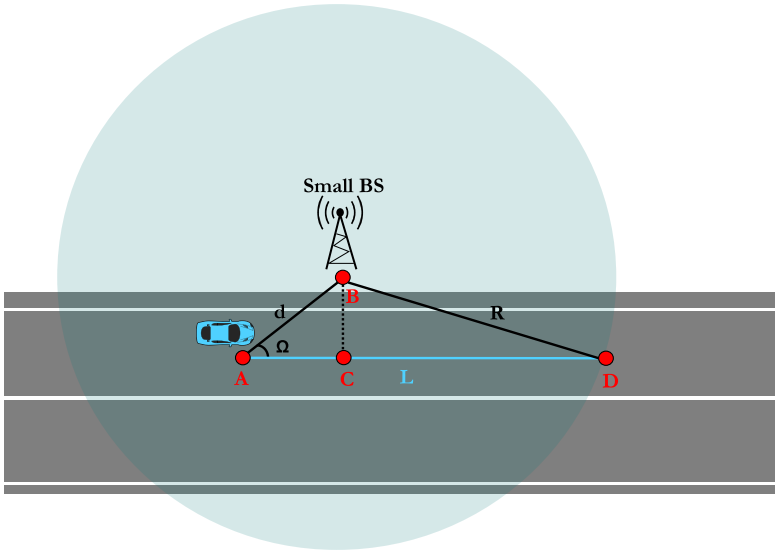

FIGURE 4. Main symbols used to prove dwell time law.

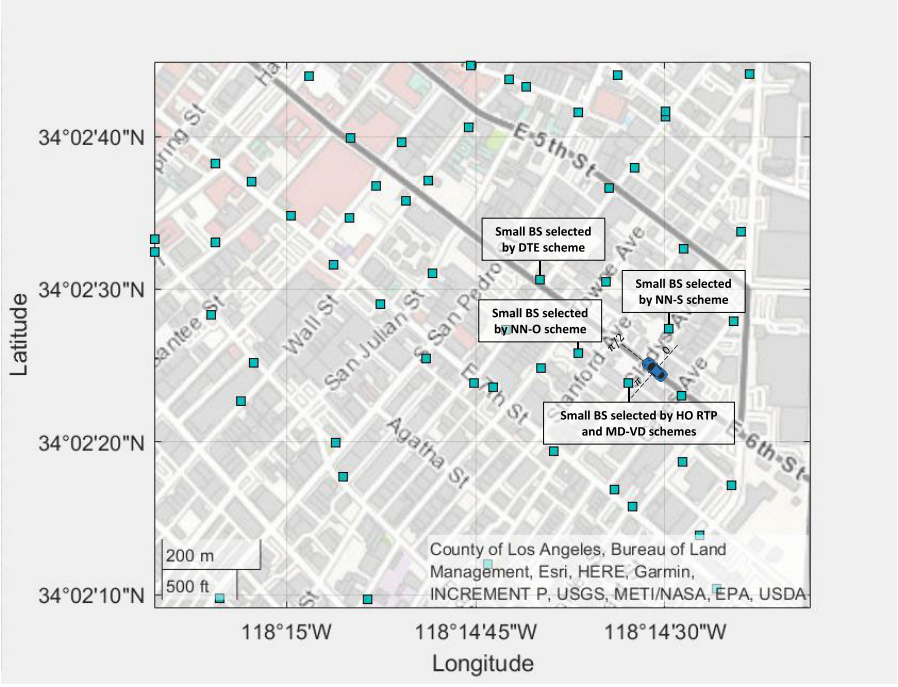

FIGURE 5. A case study of the cell selection process.

achieved data rate is positively affected by reducing the number of HOs due to handover latency. Since network energy efficiency depends on the total achieved data rates divided by the total consumed energy, the mean energy efficiency will be improved.

- Reduce downlink delay: When the vehicle moves forward, it will reach the center of the associated cell, where the propagation delay is minimal. In the other approaches, this minimum propagation delay value may not be achieved. Thus, the average downlink delay will be reduced.

IV. SYSTEM MODEL

A. DATASETS

Two datasets were used in this study; one for 5G small cells and the other for vehicles.

- **LA 5G small cells dataset:** This dataset contains 1,796 5G small base stations that are attached to streetlight poles in the city of Los Angeles. It is published by data.LAcity.org, which is the main website for LA [46]. Metadata was created on November 10, 2020 and it was updated on October 8, 2021 [47]. It consists of two columns, as shown in figure 6: the geometry of SBSs (*the_geom*) and small BS identifiers (*SLID*). The column *the_geom* includes the latitude and longitude coordinates of the small BSs.

1 the_geom	2 SLID
'POINT (-118.47984122061212 33.99493073954338)'	33003
'POINT (-118.42829045029124 33.91778721274849)'	99343
'POINT (-118.43456365854558 33.93071790544556)'	181891
'POINT (-118.43338129553185 33.93874187459162)'	150238
'POINT (-118.43322897569169 33.9523389283111)'	201351
'POINT (-118.4486922108024 33.958175132494574)'	207414
'POINT (-118.43605851733948 33.97887328658695)'	135685
'POINT (-118.46654867352007 33.97935752685767)'	81663
'POINT (-118.45925751769904 33.98388908497502)'	81642
'POINT (-118.45915736893491 33.9969446017741)'	170542

FIGURE 6. A snapshot of the LA small BSs dataset.

- **LA ehicle dataset:** This dataset is introduced by Cho and Kim in [48] and is based on real data that were collected in the city of Los Angeles on February 13, 2017. It contains a large number of samples, a total of 128,199. A snapshot of the dataset is given in figure 7. As shown in Table 2, the vehicle dataset contains data of five types of sensors, which are the global positioning system (GPS) sensor and other sensors (acceleration, orientation, gyroscope, and magnetic field). Furthermore, the dataset has video data to serve multimedia studies. The MediaQ platform, which consists of a server and a smart phone application, was used to collect, organize and share the vehicle dataset in Los Angeles. The MediaQ application was used to record sensor data while a vehicle was moving and to capture video clips simultaneously. This dataset is used because it was designed for researchers to study and analyze vehicle movements. Furthermore, the data were collected in LA, which is our study case. Also, it includes different driving roads, conditions, and other data, such as speed and azimuth angle, which make it suitable for use in this study.

We study the correlation between the stored samples in the LA 5G small cells and vehicle datasets. We found that the number of vehicles in the LA vehicle dataset that can receive signals from the small BSs stored in the LA 5G small cells dataset is 68,674, which represents 53.57% of the vehicle samples. Table 3 shows the numbers and percentages of vehicles that can and cannot receive signals from small BSs; this study considers the sample vehicles that are able to receive signals from the small BSs in the LA dataset.

B. NETWORK MODELING

The city of LA is the case study in this paper. The LA 5G small cells and vehicles datasets are used to model 5G ulta-dense network. Figure 8 shows the LA system model. It is assumed that the coverage of small cells is a circular region.

C. PROPAGATION MODEL

As defined in the 3rd Generation Partnership Project (3GPP) technical report 38.901 in [49] version 16.1.0, the 3GPP path loss model is used in this study, which is based on 5G mmWave communication. Specifically, the urban microcell-line-of-sight (UMi-LOS) model for the street canyon model is used; in the UMi environment, small BSs are lower than the tall buildings surrounding them. The formula of the UMi-LOS (street canyon) model is shown in equation (8).

$$\zeta(d)_{UMi-LOS} = \begin{cases} \zeta_1(d) & 10\ m \leqslant d \leqslant d'_{BP} \\ \zeta_2(d) & d'_{BP} \leqslant d \leqslant 5\ km \end{cases} \tag{8}$$

$$\zeta_1(d) = 32.4 + 21\ log_{10}(d) + 20\ log_{10}(f_c) \tag{9}$$

$$\zeta_2(d) = 32.4 + 40\ log_{10}(d) + 20\ log_{10}(f_c) - 9.5\ log_{10}((d'_{BP})^2 + (h_{SBS} - h_{Veh})^2) \tag{10}$$

where d is the distance between a vehicle and a small BS in meters and f_c is the carrier frequency in GHz. The breakpoint distance is denoted by d'_{BP} and its formula is represented in equation (11). The height of the small BS and the vehicle are denoted by h_{SBS} and h_{Veh}, respectively. The effective height of the small BS antenna is represented by h'_{SBS} (equation (12)), while the effective vehicle height is denoted by h'_{Veh} (equation (13)), where h_{eff} is the effective height, equalling 1 meter in the UMi environment. The speed of light in free space is denoted by c, which has a value of $3 \times 10^8\ m/s$.

$$d'_{BP} = 4\ h'_{SBS}\ h'_{Veh}\ f_c/c \tag{11}$$

$$h'_{SBS} = h_{SBS} - h_{eff} \tag{12}$$

$$h'_{Veh} = h_{Veh} - h_{eff} \tag{13}$$

The wireless channel between a vehicle and its associated small BS is modeled as a mixture of unit-mean Rayleigh-fading and log-normal shadowing.

V. PERFORMANCE ANALYSIS

A. PERFORMANCE METRICS

The performance metrics that are used to evaluate our DTE schemes are the mean of dwell time, number of horizontal HOs, achievable downlink throughput, network energy efficiency, and number of HO failures and unnecessary HOs. The mean dwell time ($E(T_d)$) and average number of horizontal HOs ($E(N_{HHO})$) are calculated based on equations (14) and (15), respectively. The number of vehicles is denoted by M and the number of horizontal HOs is represented by N_{HHO}.

$$E(T_d) = \frac{\sum_M (\sum (T_d)/N_{HHO})}{M} \tag{14}$$

$$E(N_{HHO}) = \frac{\sum_M N_{HHO}}{M} \tag{15}$$

1 kspeed	2 accSpeed	3 d_sec	4 accdist	5 sentime	6 azimuth	7 pitch	8 roll	9 light	10 gps_lat	11 gps_lon
32.2459	36.8370	1	1.2484e+04	08:53:38	30.6057	-0.8940	90.9517	52	33.9978	-118.2478
32.2459	36.6916	1	1.2484e+04	08:53:38	30.4860	-4.3319	93.6119	48	33.9978	-118.2478
32.2459	37.4577	1	1.2484e+04	08:53:38	28.4789	6.8480	98.1805	46	33.9978	-118.2478
32.2459	38.1019	1	1.2484e+04	08:53:38	29.2333	5.2237	94.9391	46	33.9978	-118.2478
32.2459	38.5656	1	1.2484e+04	08:53:38	32.4211	4.7818	80.7384	46	33.9978	-118.2478
33.0775	38.4246	1	1.2500e+04	08:53:39	29.5657	-3.7600	96.5815	48	33.9979	-118.2478
33.0775	37.5200	1	1.2500e+04	08:53:39	32.2396	-15.4392	91.1292	50	33.9979	-118.2478
33.0775	36.6851	1	1.2500e+04	08:53:39	31.0068	-11.7665	95.0702	49	33.9979	-118.2478
33.0775	36.6626	1	1.2500e+04	08:53:39	27.2035	-2.7640	103.7518	49	33.9979	-118.2478
33.0775	35.8059	1	1.2500e+04	08:53:39	30.4661	-11.8207	96.1272	50	33.9979	-118.2478

FIGURE 7. A snapshot of the LA vehicle dataset.

TABLE 2. Description of the LA vehicle dataset.

Data	**GPS Sensor Data**	· Timestamp/ Timezone Offset (in +hh:mm or -hh:mm format)
		· Latitude/ Longitude/ Altitude/ GPS Accuracy
		· Speed (it is calculated based on GPS coordinates)
	Other Sensors Data	· Timestamp/ Timezone Offset (in +hh:mm or -hh:mm format)
		· Acceleration (x, y, z)
		· Orientation (azimuth, pitch, roll)
		· Gyroscope (x, y, z)
		· MagneticField (x, y, z)
	Video Data	· Movement video clips (in MP4 format)
Driving Time		22.4 h
Driving Distance		731.6 miles (1,177.4 km)
Driving Conditions		Regular Driving, Abnormal Driving, Passing Speed Bump, Passing Uneven Road, and Passing Pothole
Driving Roads		Residential streets, urban local roads, high speed freeways, and traffic congested areas
Number of Samples		128,199

TABLE 3. The correlation between the vehicle and small cell datasets.

	Number	Percentage
Vehicles that can receive signals	68,674	53.57%
Vehicles that cannot receive signals	59,525	46.43%

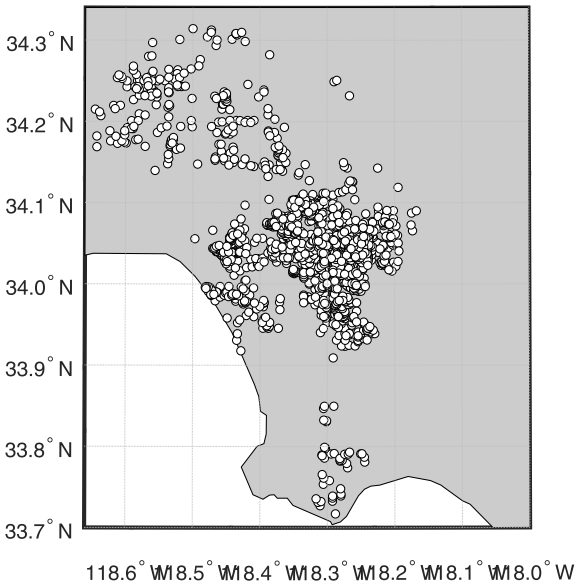

FIGURE 8. System model of LA.

The throughput of a vehicle V_m is obtained by summing the effective data rate achieved by the vehicle over the network [43], as given in equation (16).

$$Throughput_m = \sum_n R_{nm}, \quad \forall\, V_m \in \mathbb{V} \;\&\; \forall\, S_n \in \mathbb{B}. \quad (16)$$

where R_{nm} is the achievable DL data rate of the vehicle V_m served by small base stations S_n. It can be calculated based on Shannon's equation, as given in equation (17).

$$R_{nm} = BW \;\; log_2(1 + \gamma_{nm}) \quad (17)$$

The signal-to-interference-plus-noise ratio (SINR) is defined as the power of the received signal from the serving BS divided by the sum of interference power from other BSs and the power of the noise [50]. The SINR at vehicle V_m associated with small base station S_n, which is expressed as γ_{nm}, can be calculated as given in equation (18). Thermal noise is considered as an additive white Gaussian noise (AWGN) with noise power spectral density (N_0), and channel bandwidth (BW).

$$\gamma_{nm} = \frac{p_{tx_n}\zeta_{nm}(d)h_{nm}}{\sum_{i\neq n}(p_{tx_i}\zeta_{im}(d)h_{im}) + N_0 BW} \quad \forall\, V_m \in \mathbb{V} \quad and \;\forall\, S_n \in \mathbb{B}. \quad (18)$$

The transmitted power of small BSs is expressed as p_{tx}. The path loss (PL), $\zeta(d)$, is based on the 3GPP PL model, as described in section IV-C. The channel gain, which is denoted by h, is composed of the effects of log-normal shadowing and Rayleigh fading.

HO failure occurs if the dwell time within a cell is less than the HO delay (τ_i) [51]. Equation (19) represents the formula of the probability of HO failures.

$$P_f = \begin{cases} \frac{2}{\pi}[\sin^{-1}(\frac{v\tau_i}{2R}) - \sin^{-1}(\frac{vT_1}{2R})] & 0 \leqslant T_1 \leqslant \tau_i \\ 0 & \tau_i < T_1 \end{cases} \quad (19)$$

$$T_1 = \frac{2R}{v} sin(sin^{-1}(\frac{v\tau_i}{2R}) - \frac{2}{\pi}P_f); \quad 0 \leqslant P_f \leqslant 1 \quad (20)$$

where v is the velocity of a vehicle and T_1 is the time threshold of HO failures. The acceptable value of P_f in this study is 0.02. The calculation of the average number of horizontal HO failures, $E(N_f)$, is presented in equation (21).

$$E(N_f) = P_f \times E(N_{HHO}) \quad (21)$$

Unnecessary HO, also known as false HO, refers to a needless process that happens when the sum of HO delays to move into (τ_i) and out (τ_o) of a small cell exceeds the dwell time in the small cell [52]. The calculation of the probability of unnecessary HO is presented in equation (22), where T_2 is the time threshold of the unnecessary HOs.

$$P_u = \begin{cases} \frac{2}{\pi}[\sin^{-1}(\frac{v(\tau_i+\tau_o)}{2R}) - \sin^{-1}(\frac{vT_2}{2R})] \\ \quad 0 \leqslant T_2 \leqslant (\tau_i + \tau_o) \\ 0 \quad (\tau_i + \tau_o) < T_2 \end{cases} \quad (22)$$

$$T_2 = \frac{2R}{v} \sin(\sin^{-1}(\frac{v(\tau_i+\tau_o)}{2R}) - \frac{2}{\pi}P_u); \quad 0 \leqslant P_u \leqslant 1 \quad (23)$$

The average number of unnecessary HO, $E(N_u)$, is calculated based on equation (24). In this work, the acceptable value of P_u is 0.04.

$$E(N_u) = P_u \times E(N_{HHO}) \quad (24)$$

Energy efficiency (EE) is a vital criterion in designing cell selection approaches. It refers to the sum of achievable data rates divided by the total consumed power [53]. Equation (25) gives the formula for the energy efficiency, measured in bits/joule.

$$EE(bits/joule) = \frac{Achievable\ throughput(bps)}{Total\ consumed\ power(watts)} \quad (25)$$

Minimizing the amount of delays is a QoS requirement for 5G networks [54]. The downlink delay of a packet is a combination of transmission, propagation, processing and queuing delays [55], [56]. It can be expressed as given in equation (26), where D_{nmk} represents the download delay of vehicle V_m when downloading packet k through small BS S_n.

$$D_{nmk} = D^{trans}_{nmk} + D^{prop}_{nmk} + D^{proc}_{nmk} + D^{queu}_{nmk} \quad (26)$$

Transmission delay, D^{trans}_{nmk}, is the packet length (L_k) divided by the available transmission rate (R_{nm}), as shown in equation (27). In this work, the file transfer protocol (FTP) model is considered, with a packet size of up to 1500 Bytes.

$$D^{trans}_{nmk} = \frac{L_k}{R_{nm}} \quad (27)$$

Propagation delay, D^{prop}_{nmk}, refers to the time required for a packet to travel between a small BS and a vehicle. It can be obtained by dividing the distance between the small BS S_n and the vehicle V_m (X_{nm}) by the speed of light (c), as given in equation (28).

$$D^{prog}_{nmk} = \frac{X_{nm}}{c} \quad (28)$$

Processing delay, D^{proc}_{nmk}, is the latency of generating the packets, which equals several microseconds [57]. Queuing delay, D^{queu}_{nmk}, is the time spent in a queue at a small base station until the packet is transmitted. We consider an M/M/1 queuing system with average traffic arrival rate λ and average service rate μ. Queuing delay is calculated based on Little's theorem, which is a well-known law in queuing theory, as shown in equation (29) [58].

$$D^{queu}_{nmk} = \frac{1}{\mu_n - \lambda_n} \quad (29)$$

The average downlink delay of the system can be calculated as given in equation (30).

$$E(D) = \frac{\sum_M(\sum D_{nmk})}{M} \quad \forall\ V_m \in \mathbb{V}\ and\ \forall\ S_n \in \mathbb{B}.$$

B. PERFORMANCE EVALUATION

The performance of the proposed DTE is evaluated in terms of the mean dwell time, number of horizontal HOs, achievable downlink throughput, number of horizontal HO failures, and unnecessary HOs, network energy efficiency, and packet delay. In addition, a comparison was made with HO RTP, MD-VD, ML-VD, NN-O, and NN-S schemes. The simulation model of LA city was performed in MATLAB R2021a. This was selected as a simulation tool due to its powerful capabilities that can be used to simulate and evaluate the performance of 5G cellular networks. The simulation parameters are presented in Table 4.

1) AVERAGE DWELL TIME AND NUMBER OF HORIZONTAL HOs

The mean dwell time and mean number of HOs are studied at different vehicle speeds (Figures 9 and 10). We found that, when the vehicle speed increases, the dwell time decreases and the average number of horizontal HOs increases; there is an inverse relationship between the dwell time and the HO rate, where the longer the dwell time, the lower the horizontal HO rate. The proposed DTE method has the longest average dwell time. The reason is that it estimates the staying time of a vehicle within the serving small cells and it selects the small cell within range that has the longest dwell time. The NN-O scheme is the second-best method in terms of the average dwell time and number of HOs because it chooses a small BS

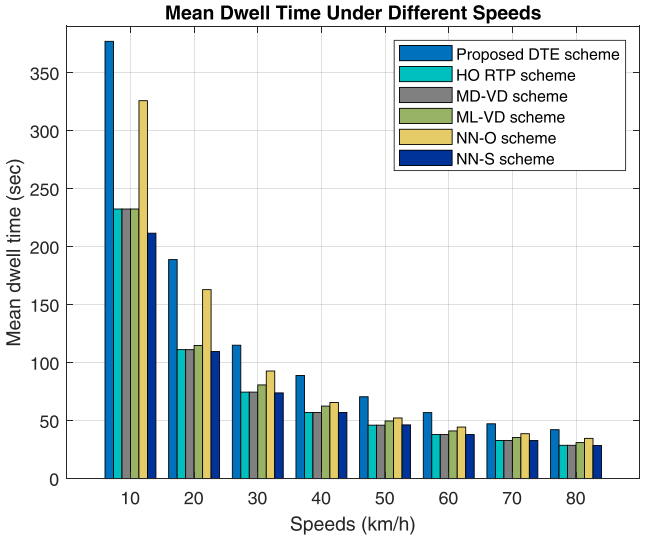

FIGURE 9. Average dwell time vs speed.

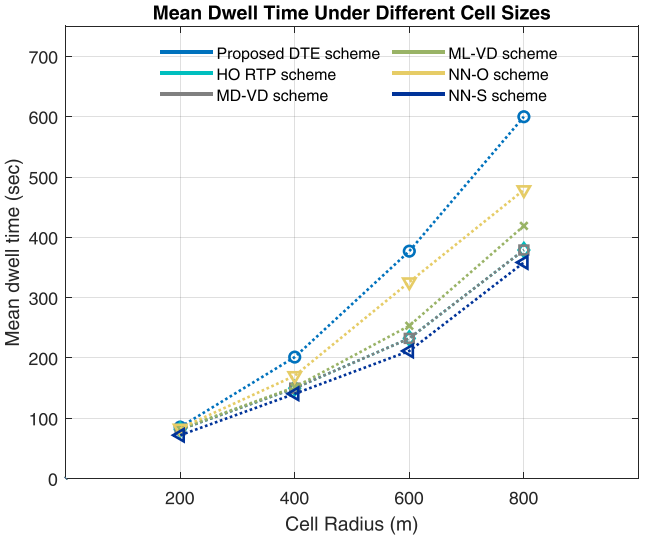

FIGURE 11. Average dwell time vs cell size.

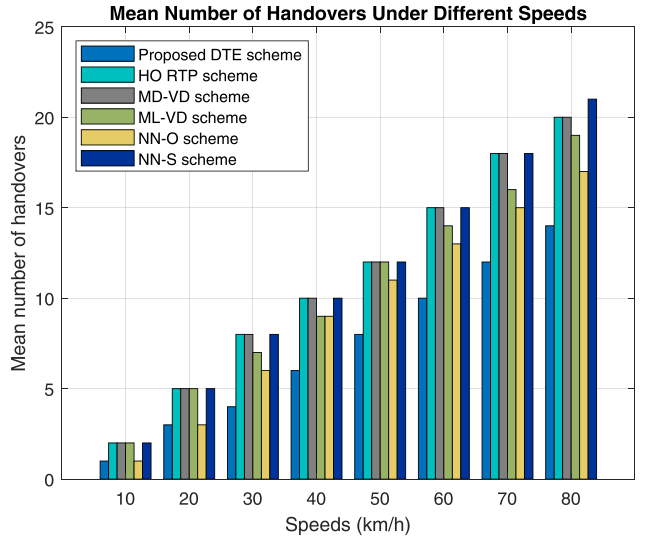

FIGURE 10. Average number of handovers vs speed.

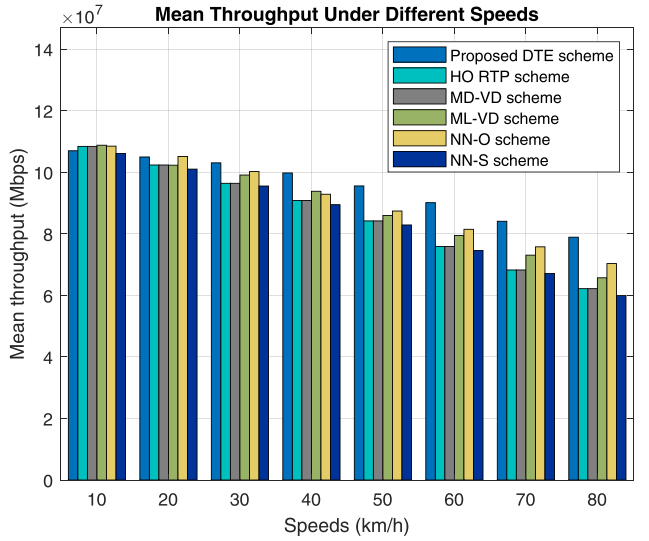

FIGURE 12. Average achievable downlink throughput vs speed.

in the vehicle direction that has the minimum azimuth in the range between $\pi/2$ and π. In other words, the selected small BS is the one that is located in the left quadrant for the vehicle with the nearest vertical line with respect to the vehicle's location. Therefore, the vehicle stays connected to the serving BS for a longer period and the average HO rate is reduced. However, the proposed DTE is superior to the NN-O scheme in terms of average dwell time and the number of horizontal HOs by 17.17% and 22.67%, respectively. Choosing the small BS with minimum azimuth within the specified range of the NN-O scheme does not necessarily lead to the longest dwell time. The ML-VD scheme depends on choosing the cell that has the minimum load in the direction of the vehicle, and therefore the cell selection will not be fixed, since it depends on the density of vehicles on the streets. The DTE method achieves superiority over the ML-VD scheme by 34.34% and 30.95% in terms of average dwell time and number of HOs, respectively; relying only on traffic load does not guarantee the longest survival of the vehicle within the serving cell. The HO RTP and MD-VD schemes have the same performance in terms of the average dwell time and the number of horizontal HOs, due to their reliance on a similar principle in choosing the serving small cell. Both schemes give high priority to the nearest cell in the direction of the vehicle, but depending on this principle will reduce the residence time and increase the number of HOs. Our DTE strategy outperforms them in terms of average number of HOs by 35.56%. The NN-S approach is the worst in terms of the average dwell time and number of HOs. Our proposed DTE protocol outperforms it by 39.42% and 36.26%, respectively. The reason behind this is that the small cell that has the minimum angle within the range between 0 to π is selected in the NN-O scheme to be

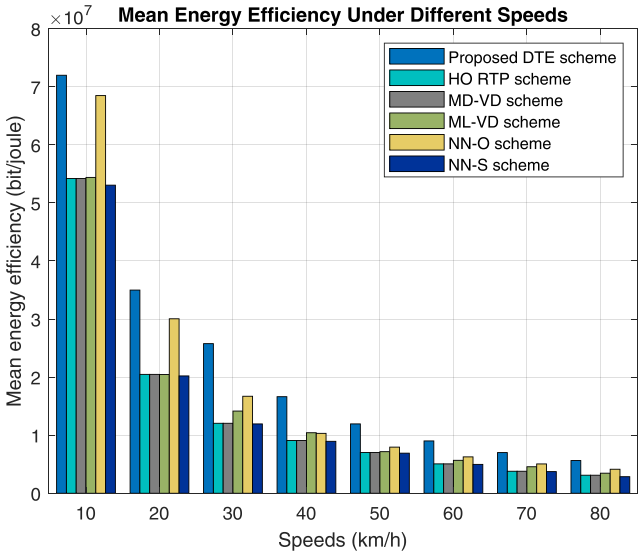

FIGURE 13. Average energy efficiency vs speed.

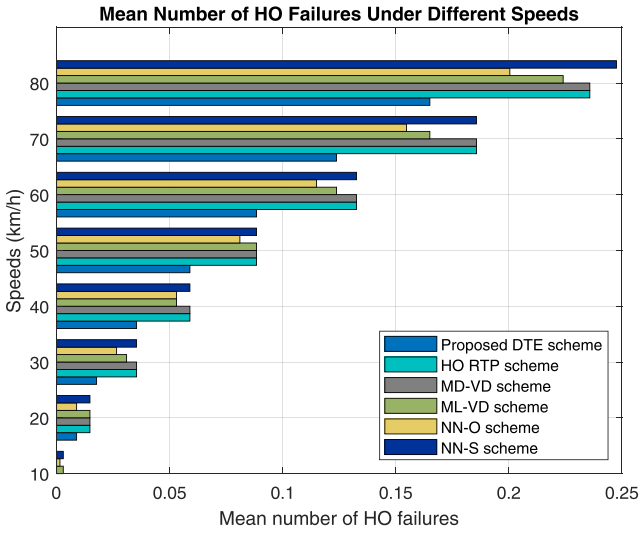

FIGURE 14. Average number of handover failures vs speed.

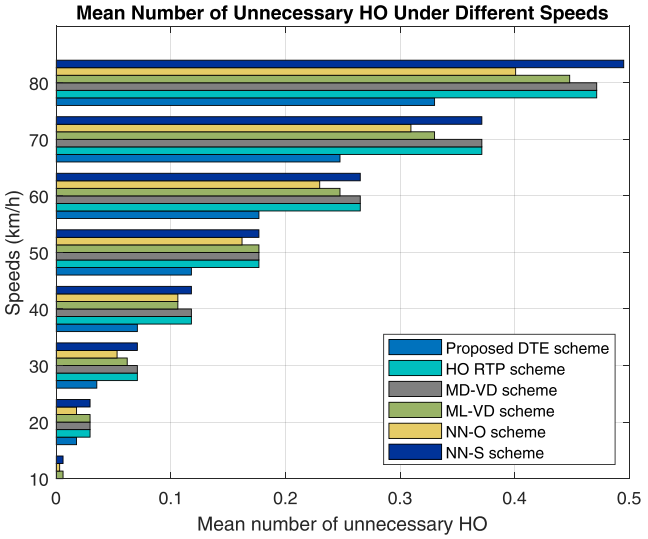

FIGURE 15. Average number of unnecessary handovers vs speed.

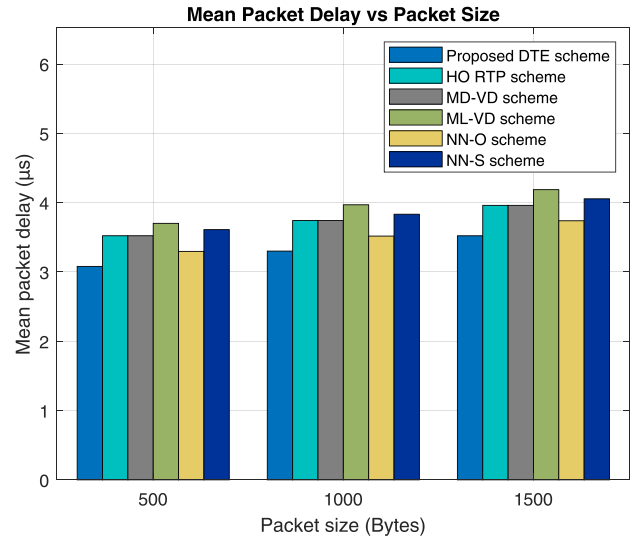

FIGURE 16. Average DL packet delay vs packet size.

the serving cell. Therefore, the cell in the right quadrant for the vehicle located on the lowest horizontal line with respect to the vehicle will be selected. Choosing the cell located on the lowest horizontal line will increase the number of HOs when the vehicle is moving forward.

Figure 11 represents the relationship between the mean dwell time under different small cell sizes, where cell radii of 200, 400, 600, and 800 meters are considered. We found that there is a direct relationship between the size of the small cell and the mean dwell time of vehicles within it. As shown in the line chart, the proposed DTE scheme outperforms the other cell selection methods because it is based on estimating the dwell time and selecting the small BS with the longest residence time. The larger the cell size, the greater the superiority of our scheme over the rest of the methods. The other cell selection schemes are ranked from the best to the worst as follows: NN-O, ML-VD, HO RTP and MD-VD, then the NN-S scheme. This result confirms what we obtained in figure 9 for the reasons discussed previously.

2) AVERAGE ACHIEVABLE DOWNLINK THROUGHPUT AND ENERGY EFFICIENCY

The relationship between the average achievable downlink throughput and vehicle speeds is shown in figure 12. The higher the vehicle speed, the lower the average DL throughput achieved by the vehicle, due to the increase in the number of horizontal handovers. Our proposed DTE made improvements over the other cell selection schemes in terms of the average downlink throughput achieved by vehicles. The reason is that relying on prolonging the dwell time has a positive effect on the achievable downlink throughput in two aspects. The first is that, when the vehicle is moving forward, the maximum data rate is reached when the vehicle reaches the middle of the cell. The other schemes do not guarantee

TABLE 4. Performance evaluation parameters.

Parameter	Symbol	Value
Number of 5G small cells	N	1,796
Small base station height (m)	h_{SBS}	10
Small cell radius (m)	R	600
Carrier frequency (GHz)	f_c	28
System bandwidth (MHz)	BW	500
Transmission power (Watt)	P_{tx}	1
Path loss model (dB)	$\zeta(d)$	3GPP UMi model (street canyon)
Shadowing standard deviation (dB)	σ_{SF}	4
Shadowing	X_{Normal}	Log-normal
Fast fading	$X_{Rayleigh}$	Rayleigh fading
Thermal noise density (dBm/Hz)	N_o	-174
Vehicle speed (km/h)	v	[10-80]
Vehicle height (m)	h_{Veh}	1.8
RSSI threshold (dBm)	Th	-100
HO delay (sec)	τ_{HO}	1
Simulation time (s)	T_{Sim}	600

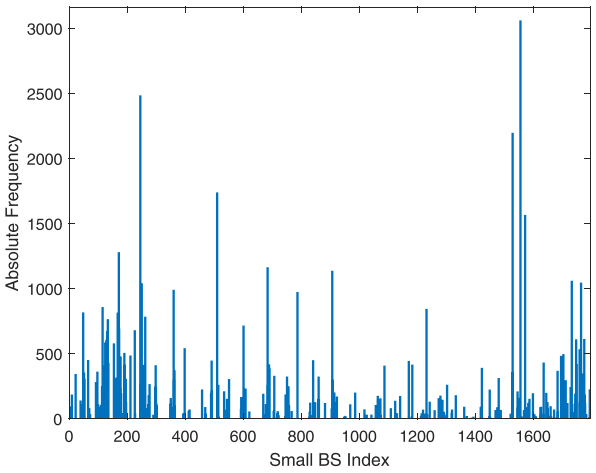

(a) Absolute Frequency.

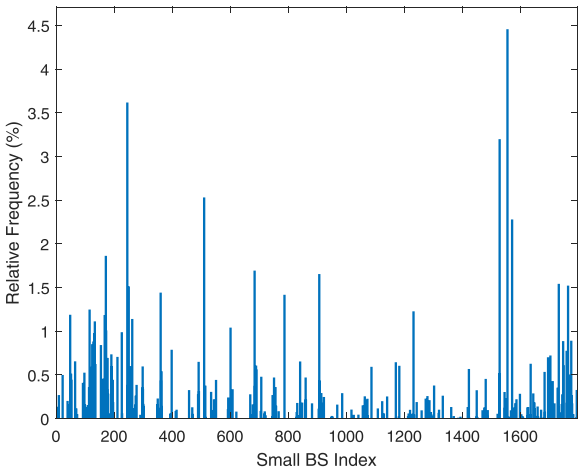

(b) Relative Frequency.

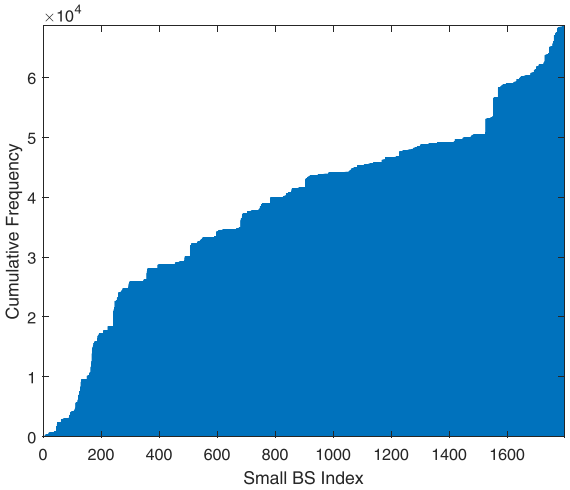

(c) Cumulative Frequency.

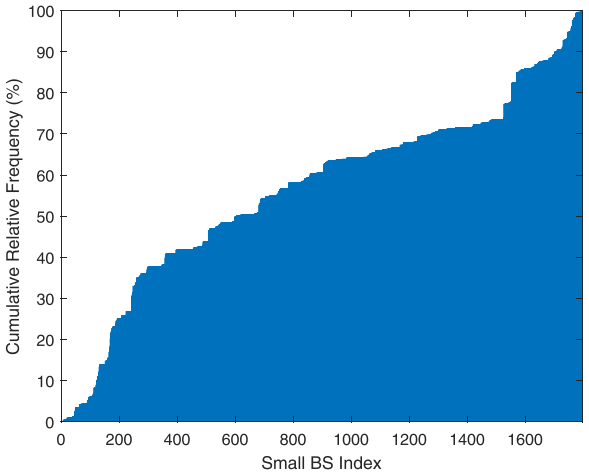

(d) Cumulative Relative Frequency.

FIGURE 17. Absolute, relative, cumulative, and cumulative relative frequencies of the LA small BSs.

reaching this maximum data rate value. The second aspect is that the handover between cells leads to reduced average throughput due to the HO latencies involved in performing the handover process. Our DTE scheme is the best scheme in terms of the number of HOs, as discussed previously. Therefore, our method is superior to HO RTP, MD-VD,

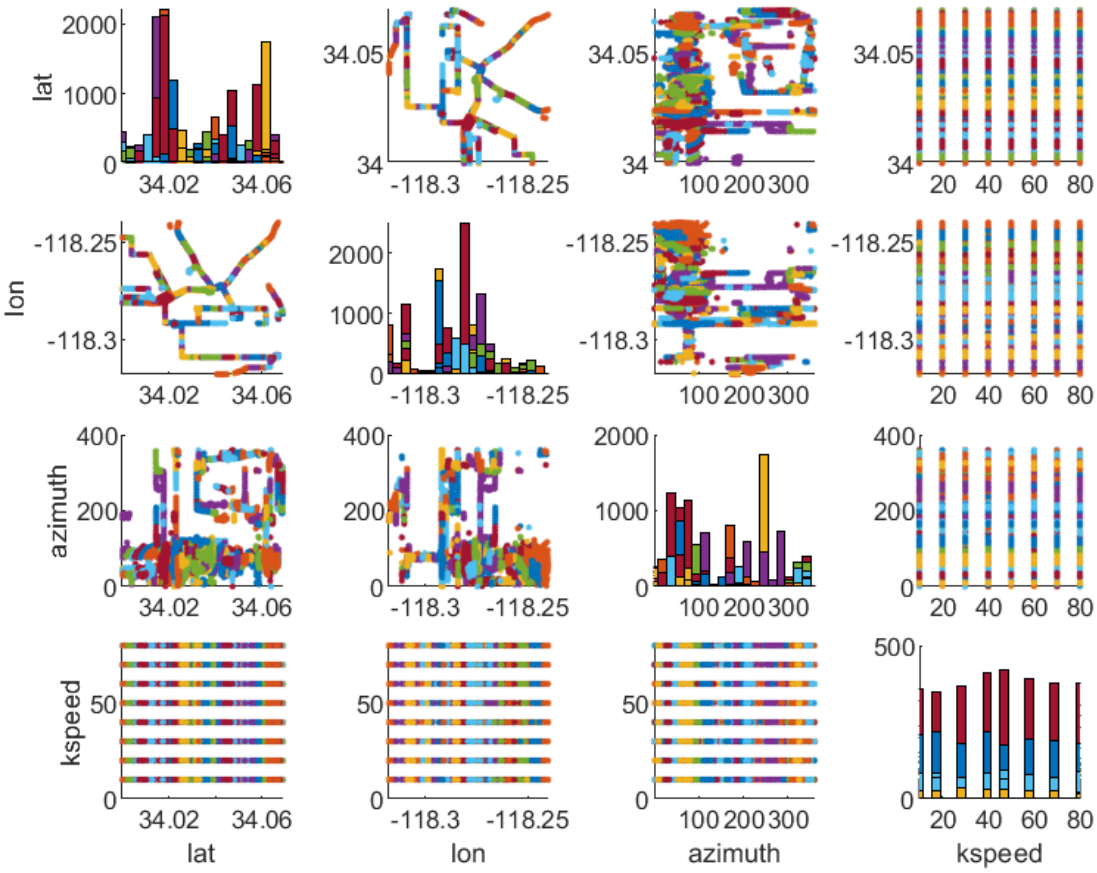

FIGURE 18. Pair plots of all variables that are used to estimate the dwell time.

ML-VD, NN-O, and NN-S schemes by 37.26%, 34.25%, 18.59%, and 38.45%, respectively.

Figure 13 represents the average network energy efficiency for vehicles under different driving speeds. As the energy efficiency is the ratio between the achievable vehicle throughput and the total consumed power, the DTE scheme is superior to the other cell selection schemes because it achieves the highest average downlink throughput.

3) AVERAGE NUMBER OF HO FAILURES AND UNNECESSARY HOs

The relationship between the average number of HO failures and unnecessary HOs versus vehicle speeds is shown in figures 14 and 15. These show that the higher the vehicle speed, the greater the number of HO failures and unnecessary HOs. This is due to the short dwell time caused by the increase in the speed of the vehicle. Reducing the average number of HOs will inevitably reduce the mean numbers of HO failures and unnecessary HOs, since both of them depend on the duration of residence within the serving cell. Based on our results, the cell selection schemes are arranged based on the average number of HOs, from highest to lowest, as NN-S, HO RTP and MD-VD, ML-VD, NN-O, then DTE, as shown in figure 10. Consequently, our proposed DTE protocol outperforms NN-S, HO RTP and MD-VD schemes by up to 33.79% and ML-VD and NN-O by 28.93% and 22.07%, respectively in terms of the average number of HO failures and unnecessary HOs.

4) AVERAGE PACKET DELAY

Figure 16 represents the mean packet delay under different packet sizes, which are 500, 1000, and 1500 Bytes. We found that there is a direct relationship between the average delay and the packet size. As the packet size increases, the corresponding downlink delay increases, due to the delay in the transmission of packets. The proposed DTE scheme achieves improvements over the other methods in terms of mean packet delay, because it decreases the average propagation delay. The propagation delay depends on the distance between the serving small BS and the associated vehicle. Under the DTE scheme, the minimum value of the propagation delay is reached when the vehicle is close to the center of the cell, while other methods may not reach this minimum value. Consequently, the DTE approach outperforms HO RTP and MD-VD by 11.78% and it has superiority over ML-VD,

NN-S and NN-O, by 16.49%, 13.88%, and 6.16%, respectively.

C. STATISTICAL ANALYSIS

In this section, we study the frequency of selecting a small base station, which is included in descriptive statistics. In addition, pair plots are represented, which are statistical plots that are used to analyze the distribution and show the dependencies between each pair of variables that are used to estimate the dwell time of a vehicle within a selected small BS.

Frequency tables are used to analyze the selection of small base stations throughout the city of LA based on the proposed cell selection scheme. Figure 17 shows absolute frequency, relative frequency, cumulative frequency, and cumulative relative frequency of the small BSs. Absolute frequency is the number of times that a small base station is selected (Figure 17a). The relative frequency is the ratio between the absolute frequency and the total number of observations (Figure 17b). The cumulative frequency is the sum of the absolute frequencies at or below a given observation (Figure 17c).The cumulative relative frequency is the cumulative frequency divided by the total number of observations (Figure 17d) [59]. Based on the frequency distribution provided above, it can be inferred that the density of vehicles that can receive signals in the LA vehicle database varies from one street to another. In some streets, there are small cells, but there are no vehicles to be associated with. Moreover, the number of the small base stations in some streets is larger than in other streets. In addition, the distribution of LA small base stations is based on the LA city infrastructure, and therefore the small cell within range is chosen which has the longest dwell time.

Pair plots are a set of scatter and histogram plots that are used to shows the dependencies between each pair of variables, and are a plot that combines all possible joined plots [60]. Figure 18 shows the pair plots of all variables that are used to estimate the dwell time of a vehicle within a serving small BS, which are latitude and longitude coordinates, azimuth, and speed of vehicles. The histogram plots on the diagonal are used to show a single variable relationship, while the scatter plots are used to represent the relationship between each two variables. As shown in the pair plots, the selection of small cells using our DTE scheme depends on the related vehicle information, in terms of their geographical location and the direction and speed of movement, and their relationship to the distribution of the small BSs. All of these factors play an important role in choosing the small cell to be associated with. In addition, we found that the vehicle samples considered are distributed in many areas in the city of Los Angeles and they are not limited to a specific region.

VI. CONCLUSION AND FUTURE WORK

In this paper, we proposed the DTE scheme as a cell selection method for 5G UDNs. It increases the dwell time of small cells to reduce the average rate of HOs and to improve the average achievable throughput and energy efficiency. The DTE algorithm passes through four steps to achieve its goals. The dwell time is estimated based on vehicle information; that is, latitude and longitude coordinates, speed, and direction. The algorithm was applied to the city of Los Angeles in California, and real vehicle information collected in LA was used. The simulation result shows that our DTE scheme outperforms other recent related schemes in terms of the average number of HOs by up to 36.26% and, therefore, reduces the average number of HO failures and unnecessary HOs. Furthermore, it made enhancements in terms of mean achievable DL throughput and energy efficiency by up to 38.45%. In addition, the average packet delay is reduced by up to 16.49%. For future work, there are several development aspects that can be considered. The proposed scheme can be enhanced to consider multi-tier heterogeneous network infrastructure that is made up of macro and small BSs, where the macro base stations are still required for high-mobility vehicles. Furthermore, machine learning (ML) techniques can be used to intelligently perform the cell selection task with reduction in computational complexity. Recurrent neural networks (RNN) and convolutional neural networks (CNN) are examples of ML-modeling techniques that can be used to predict the best BS to be associated with. Moreover, software-defined networking can be applied to centrally coordinate the cell association decision and to ease the network management process.

APPENDIX A
PROOF OF THE DWELL TIME LEMMA

Proof: We start the proof of dwell time (T_d) of a vehicle in a small cell by relying on the symbols shown in figure 4. The radius of the small cell is denoted by R and d is the distance between the current location of a vehicle and the small BS. The angle between the vehicle direction and SBS is represented by Ω. The length of the line L, which is the dwell distance, equals the sum of the lengths of the two lines that form it (AC and CD). Therefore, it can be represented as

$$L = AC + CD \tag{30}$$

By considering the sides and angle Ω of the triangle ABC and by using the cosine and sine rules, we obtain

$$AC = d\ cos(\Omega) \tag{31}$$

$$BC = d\ sin(\Omega) \tag{32}$$

Pythagoras's theorem was applied to the triangle BCD to find the length of the second segment of line L, which is CD, and we obtain

$$\begin{aligned} (BD)^2 &= (BC)^2 + (CD)^2 \\ R^2 &= d^2\ sin^2(\Omega) + (CD)^2 \\ CD &= \sqrt{R^2 - d^2\ sin^2(\Omega)} \end{aligned} \tag{33}$$

By substituting equations (31) and (33) into equation (30), we get

$$L = d\ cos(\Omega) + \sqrt{R^2 - d^2\ sin^2(\Omega)} \tag{34}$$

Finally, since dwell time (T_d) in the small cell equals dwell distance (L) divided by the velocity of the vehicle (v), we get:

$$T_d = \frac{d\ cos(\Omega) + \sqrt{R^2 - d^2\ sin^2(\Omega)}}{v} \tag{35}$$

APPENDIX B
LIST OF ABBREVIATIONS

Table 5 gives a list of abbreviations.

TABLE 5. List of abbreviations.

Abbreviation	Description
3GPP	Third Generation Partnership Project
5G	Fifth-Generation
AS	Active Set
BS	Base Station
CNN	Convolutional Neural Network
CoMP	Coordinated Multipoint
C-RAN	Centralized Radio Access Network
DCS	Dynamic Cell Selection
DTE	Dwell Time Estimation
GPS	Global Positioning System
HO	Handover
HO RTP	Handover based on Residence Time Prediction
HUDN	Heterogeneous Ultra-Dense Network
iMACH	improved MACH
IoT	Internet of Things
ISD	Inter-Site Distance
LA	Los Angeles
MACH	Movement Aware CoMP Handover
MD-VD	Minimum Distance in the Vehicle Direction
ML-VD	Minimum Load in the Vehicle Direction
mMIMO	massive Multiple-Input Multiple-Output
mmWave	millimeter-Wave
NFV	Network Function Virtualization
NN-O	Next Neighbor on the Opposite street
NN-S	Next Neighbor on the Same street
PF	Proportional Fairness
PPP	Poisson point processes
QoS	Quality of Service
RLFs	Radio Link Failures
RNN	Recurrent Neural Network
RSRP	Reference Signal Receiving Power
RSSI	Received Signal Strength Indicator
SBS	Small Base Station
SDN	Software Defined Networking
SINR	Signal-to-Interference-plus-Noise Ratio
TOPSIS	Technique for Order Preference by Similarity to Ideal Solution
TPs	Transmit Points
UDN	Ultra-Dense Network
UE	User Equipment
UMi-LOS	Urban Micro cell-Line of Sight
V2N	Vehicle-to-Network
V2P	Vehicle-to-Pedestrians
V2V	Vehicle-to-Vehicle
V2X	Vehicle-to-Everything

CONFLICTS OF INTEREST

The authors declare no conflict of interest.

ACKNOWLEDGMENT

The authors would like to thank the Deanship of Scientific Research and RSSU at King Saud University for their technical support.

REFERENCES

[1] Ł. Januszkiewicz, P. Di Barba, Ł. Jopek, and S. Hausman, "Many-objective automated optimization of a four-band antenna for multiband wireless sensor networks," *Sensors*, vol. 18, no. 10, p. 3309, Oct. 2018.

[2] I. Alablani and M. Alenazi, "Performance evaluation of sensor deployment strategies in WSNs towards IoT," in *Proc. IEEE/ACS 16th Int. Conf. Comput. Syst. Appl. (AICCSA)*, Nov. 2019, pp. 1–8.

[3] L. Nkenyereye, L. Nkenyereye, S. M. R. Islam, Y.-H. Choi, M. Bilal, and J.-W. Jang, "Software-defined network-based vehicular networks: A position paper on their modeling and implementation," *Sensors*, vol. 19, no. 17, p. 3788, Aug. 2019.

[4] L. Guevara and F. A. Cheein, "The role of 5G technologies: Challenges in smart cities and intelligent transportation systems," *Sustainability*, vol. 12, no. 16, p. 6469, Aug. 2020.

[5] F. Arena, G. Pau, and A. Severino, "V2X communications applied to safety of pedestrians and vehicles," *J. Sensor Actuator Netw.*, vol. 9, no. 1, p. 3, Dec. 2019.

[6] A. Martínez, E. Cañibano, and J. Romo, "Analysis of low cost communication technologies for V2I applications," *Appl. Sci.*, vol. 10, no. 4, p. 1249, Feb. 2020.

[7] C. Storck and F. Duarte-Figueiredo, "A 5G V2X ecosystem providing internet of vehicles," *Sensors*, vol. 19, no. 3, p. 550, Jan. 2019.

[8] M. Das and A. Kumar, "Introduction to 5G telecommunication network," in *CMOS Analog IC Design for 5G Beyond*. Berlin, Germany: Springer, 2021, pp. 1–13.

[9] L. Dash and M. Khuntia, "A survey on various security issues for 5G mobile networks in WSN," in *Intelligent and Cloud Computing*. Springer, 2021, pp. 669–679.

[10] M. Vaezi and Y. Zhang, "Radio access network evolution," in *Cloud Mobile Networks*. Berlin, Germany: Springer, 2017, pp. 67–86.

[11] J. An, K. Yang, J. Wu, N. Ye, S. Guo, and Z. Liao, "Achieving sustainable ultra-dense heterogeneous networks for 5G," *IEEE Commun. Mag.*, vol. 55, no. 12, pp. 84–90, Dec. 2017.

[12] K. Xiao, W. Li, M. Kadoch, and C. Li, "On the secrecy capacity of 5G mmWave small cell networks," *IEEE Wireless Commun.*, vol. 25, no. 4, pp. 47–51, Aug. 2018.

[13] Y. Ren, W. Yang, X. Zhou, H. Chen, and B. Liu, "A survey on TCP over mmWave," *Comput. Commun.*, vol. 171, pp. 80–88, Apr. 2021.

[14] P. Deb, A. Mukherjee, and D. De, "A study of densification management using energy efficient femto-cloud based 5G mobile network," *Wireless Pers. Commun.*, vol. 101, no. 4, pp. 2173–2191, Aug. 2018.

[15] D. Muirhead, M. A. Imran, and K. Arshad, "A survey of the challenges, opportunities and use of multiple antennas in current and future 5G small cell base stations," *IEEE Access*, vol. 4, pp. 2952–2964, 2016.

[16] X. Ge, S. Tu, G. Mao, and C. X. Wang, "5G ultra-dense cellular networks," *IEEE Trans. Wireless Commun.*, vol. 23, no. 1, pp. 72–79, Feb. 2016.

[17] H. Zhang, M. Min, L. Xiao, S. Liu, P. Cheng, and M. Peng, "Reinforcement learning-based interference control for ultra-dense small cells," in *Proc. IEEE Global Commun. Conf. (GLOBECOM)*, Dec. 2018, pp. 1–6.

[18] D. Calabuig, S. Barmpounakis, S. Gimenez, A. Kousaridas, T. R. Lakshmana, J. Lorca, P. Lunden, Z. Ren, P. Sroka, E. Ternon, V. Venkatasubramanian, and M. Maternia, "Resource and mobility management in the network layer of 5G cellular ultra-dense networks," *IEEE Commun. Mag.*, vol. 55, no. 6, pp. 162–169, Jun. 2017.

[19] A. K. Danburam, M. A. Gadam, A. D. Usman, and S. M. Sani, "Energy-efficient bias-based user association for heterogeneous networks in LTE-Advanced," in *Advances on Computational Intelligence in Energy*. Berlin, Germany: Springer, 2019, pp. 147–168.

[20] T. Zhou, N. Jiang, Z. Liu, and C. Li, "Joint cell activation and selection for green communications in ultra-dense heterogeneous networks," *IEEE Access*, vol. 6, pp. 1894–1904, 2018.

[21] B. Li, H. Zhang, P. Hao, and J. Li, "Sojourn time estimation-based small cell selection in ultra-dense networks," in *Proc. IEEE 28th Annu. Int. Symp. Pers., Indoor, Mobile Radio Commun. (PIMRC)*, Oct. 2017, pp. 1–5.

[22] M. Naresh, D. V. Reddy, and K. R. Reddy, "A comprehensive study on vertical handover for IEEE 802.21 wireless networks," in *Proc. 4th Int. Conf. I-SMAC (IoT Social, Mobile, Analytics Cloud) (I-SMAC)*, Oct. 2020, pp. 343–347.

[23] L. Tuyisenge, M. Ayaida, S. Tohme, and L.-E. Afilal, "A mobile internal vertical handover mechanism for distributed mobility management in VANETs," *Veh. Commun.*, vol. 26, Dec. 2020, Art. no. 100277.

[24] I. A. Alablani and M. A. Arafah, "An adaptive cell selection scheme for 5G heterogeneous ultra-dense networks," *IEEE Access*, vol. 9, pp. 64224–64240, 2021.

[25] S. Natarajan, T. Khandelwal, and M. Mittal, "MEC enabled cell selection for micro-operators based 5G open network deployment," in *Proc. IEEE Wireless Commun. Netw. Conf. Workshops (WCNCW)*, Apr. 2020, pp. 1–5.

[26] Y. M. Waheidi, M. Jubran, and M. Hussein, "User driven multiclass cell association in 5G HetNets for mobile & IoT devices," *IEEE Access*, vol. 7, pp. 82991–83000, 2019.
[27] Y. Yang, J. Xu, G. Shi, and C.-X. Wang, *5G Wireless Systems*. Berlin, Germany: Springer, 2018.
[28] R. Abdullah and Z. Zukarnain, "Enhanced handover decision algorithm in heterogeneous wireless network," *Sensors*, vol. 17, no. 7, p. 1626, Jul. 2017.
[29] Ctia.Org. *What is a Small Cell? A Brief Explainer*. Accessed: Jan. 3, 2021. [Online]. Available: https://www.ctia.org/news/what-is-a-small-cell
[30] R. Zhou, X. Zhang, S. Qin, J. C. S. Lui, Z. Zhou, H. Huang, and Z. Li, "Online task offloading for 5G small cell networks," *IEEE Trans. Mobile Comput.*, early access, Nov. 6, 2020, doi: 10.1109/TMC.2020.3036390.
[31] S. Pincetl, R. Graham, S. Murphy, and D. Sivaraman, "Analysis of high-resolution utility data for understanding energy use in urban systems: The case of los Angeles, California," *J. Ind. Ecol.*, vol. 20, no. 1, pp. 166–178, Feb. 2016.
[32] P. Connerton, J. V. de Assunção, R. M. De Miranda, A. D. Slovic, P. J. Pérez-Martínez, and H. Ribeiro, "Air quality during COVID-19 in four megacities: Lessons and challenges for public health," *Int. J. Environ. Res. Public Health*, vol. 17, no. 14, p. 5067, Jul. 2020.
[33] Data.Gov. (Dec. 2020). *Small Cell Locations*. Accessed: Jan. 3, 2021. [Online]. Available: https://catalog.data.gov/dataset/small-cell-locations-95385
[34] I. A. Alablani and M. A. Arafah, "Enhancing 5G small cell selection: A neural network and IoV-based approach," *Sensors*, vol. 21, no. 19, p. 6361, Sep. 2021.
[35] A. Alhammadi, M. Roslee, M. Y. Alias, I. Shayea, and S. Alraih, "Dynamic handover control parameters for LTE–A/5G mobile communications," in *Proc. Adv. Wireless Opt. Commun. (RTUWO)*, Nov. 2018, pp. 39–44.
[36] F. B. Tesema, A. Awada, I. Viering, M. Simsek, and G. P. Fettweis, "Fast cell select for mobility robustness in intra-frequency 5G ultra dense networks," in *Proc. IEEE 27th Annu. Int. Symp. Pers., Indoor, Mobile Radio Commun. (PIMRC)*, Sep. 2016, pp. 1–7.
[37] S. Kapoor, D. Grace, and T. Clarke, "A base station selection scheme for handover in a mobility-aware ultra-dense small cell urban vehicular environment," in *Proc. IEEE 28th Annu. Int. Symp. Pers., Indoor, Mobile Radio Commun. (PIMRC)*, Oct. 2017, pp. 1–5.
[38] N. Naderializadeh, H. Nikopour, O. Orhan, and S. Talwar, "Feedback-based interference management in ultra-dense networks via parallel dynamic cell selection and link scheduling," in *Proc. IEEE Int. Conf. Commun. (ICC)*, May 2018, pp. 1–6.
[39] Q. Liu, C. F. Kwong, S. Zhang, L. Li, and J. Wang, "A fuzzy-clustering based approach for MADM handover in 5G ultra-dense networks," *Wireless Netw.*, pp. 1–14, Sep. 2019.
[40] A. Khodmi, S. B. Rejeb, N. Agoulmine, and Z. Choukair, "A joint power allocation and user association based on non-cooperative game theory in an heterogeneous ultra-dense network," *IEEE Access*, vol. 7, pp. 111790–111800, 2019.
[41] H. T. Nguyen, H. Murakami, K. Nguyen, K. Ishizu, F. Kojima, J. D. Kim, S. H. Chung, and W. J. Hwang, "Joint user association and power allocation for millimeter-wave ultra-dense networks," *Mobile Netw. Appl.*, vol. 25, no. 1, pp. 274–284, Feb. 2020.
[42] Y. Zhang, L. Xiong, and J. Yu, "Deep learning based user association in heterogeneous wireless networks," *IEEE Access*, vol. 8, pp. 197439–197447, 2020.
[43] W. Sun, L. Wang, J. Liu, N. Kato, and Y. Zhang, "Movement aware CoMP handover in heterogeneous ultra-dense networks," *IEEE Trans. Commun.*, vol. 69, no. 1, pp. 340–352, Jan. 2021.
[44] Z. Qin, W. Feng, Z. Yue, and H. Tian, "A handover management strategy using residence time prediction in 5G ultra-dense networks," in *Signal and Information Processing, Networking and Computers*. Berlin, Germany: Springer, 2021, pp. 808–816.
[45] A. N. Mian, T. Liaqat, and A. Hameed, "A fresh look into the handoff mechanism of IEEE 802.11s under mobility," in *Proc. IEEE 86th Veh. Technol. Conf. (VTC-Fall)*, Sep. 2017, pp. 1–5.
[46] Data.Lacity.Org. *Small Cell Locations*. Accessed: Oct. 10, 2021. [Online]. Available: https://https://data.lacity.org/City-Infrastructure-Service-Requests/Sm%all-Cell-Locations/3nrm-mq6k
[47] Catalog.Data.Gov. *Small Cell Locations*. Accessed: Oct. 10, 2021. [Online]. Available: https://catalog.data.gov/dataset/small-cell-locations
[48] W. Cho and S. H. Kim, "Multimedia sensor dataset for the analysis of vehicle movement," in *Proc. 8th ACM Multimedia Syst. Conf.*, Jun. 2017, pp. 175–180, doi: 10.1145/3083187.3083217.
[49] *Study on Channel Model for Frequencies From 0.5 to 100 GHz (Release 16)*, Standard ETSI TR 138 901 V14.0.0, in 3rd Generation Partnership Project; Technical Specification Group Radio Access Network; Study on Channel Model for Frequencies From 0.5 to 100 GHz (Release 16), 3GPP, 2019.
[50] M. Bakshi, B. Jaumard, and L. Narayanan, "Optimal aggregated ConvergeCast scheduling with an SINR interference model," in *Proc. IEEE 13th Int. Conf. Wireless Mobile Comput., Netw. Commun. (WiMob)*, Oct. 2017, pp. 1–8.
[51] X. Yan, Y. A. Sekercioglu, and N. Mani, "A method for minimizing unnecessary handovers in heterogeneous wireless networks," in *Proc. Int. Symp. World Wireless, Mobile Multimedia Netw.*, Jun. 2008, pp. 1–5.
[52] R. Hussain, S. A. Malik, S. Abrar, R. A. Riaz, H. Ahmed, and S. A. Khan, "Vertical handover necessity estimation based on a new dwell time prediction model for minimizing unnecessary handovers to a WLAN cell," *Wireless Pers. Commun.*, vol. 71, no. 2, pp. 1217–1230, Jul. 2013.
[53] M. Javad-Kalbasi, Z. Naghsh, M. Mehrjoo, and S. Valaee, "A new heuristic algorithm for energy and spectrum efficient user association in 5G heterogeneous networks," in *Proc. IEEE 31st Annu. Int. Symp. Pers., Indoor Mobile Radio Commun.*, Aug. 2020, pp. 1–7.
[54] M. J. F. Alenazi, A. Almutairi, S. Almowuena, A. Wadood, and E. K. Cetinkaya, "NFV provisioning in large-scale distributed networks with minimum delay," *IEEE Access*, vol. 8, pp. 151753–151763, 2020.
[55] O. A. Egaji, A. Griffiths, and M. S. Hasan, "Delay optimisation for multimedia application in a wireless network control system (WNCS)," in *Proc. 11th IEEE Annu. Inf. Technol., Electron. Mobile Commun. Conf. (IEMCON)*, Nov. 2020, pp. 267–275.
[56] I. Alablani and M. Alenazi, "EDTD-SC: An IoT sensor deployment strategy for smart cities," *Sensors*, vol. 20, no. 24, p. 7191, Dec. 2020.
[57] Y. Zhong, M. Haenggi, F.-C. Zheng, W. Zhang, T. Q. S. Quek, and W. Nie, "Toward a tractable delay analysis in ultra-dense networks," *IEEE Commun. Mag.*, vol. 55, no. 12, pp. 103–109, Dec. 2017.
[58] H. Chen, Q. Chen, R. Chai, and D. Zhao, "Utility function optimization based joint user association and content placement in heterogeneous networks," in *Proc. 9th Int. Conf. Wireless Commun. Signal Process. (WCSP)*, Oct. 2017, pp. 1–6.
[59] J. A. L. Vázquez, J.-L. Casteleiro-Roca, E. Jove, F. Zayas-Gato, H. Quintián, and J. L. Calvo-Rolle, "Data collection description for evaluation and analysis of engineering students academic performance," in *Proc. Int. Conf. Eur. Transnational Educ.* Berlin, Germany: Springer, 2020, pp. 317–328.
[60] M. Mohammad-Amini, B. Einabadi, A. Baboli, and R. Tavakkoli-Moghaddam, "Determination of health key performance indicators and their visualization in the production system in the context of industry 4.0," in *Proc. IEEE 8th Int. Conf. Ind. Eng. Appl. (ICIEA)*, Apr. 2021, pp. 126–131.

IBTIHAL AHMED ALABLANI received the B.S. degree in Computer Science from Princess Nourah Bint Abdulrahman University, in 2008, and the M.S. degree in Computer Engineering from King Saud University, in 2013, where she is currently pursuing the Ph.D. degree with the Computer Engineering Department. Since 2008, she has been working at Technical and Vocational Training Corporation (TVTC), Technical College, as a Faculty Member. Her research interests include wireless sensor networks, 5G heterogeneous networks, smart cities, and machine learning. She was awarded a certificate of excellence from the Saudi Ministry of Education as one of the top students in Saudi Arabia at High School, in 2004.

MOHAMMED AMER ARAFAH received the B.S. degree from King Saud University and the M.S. and Ph.D. degrees from the University of Southern California, USA. He is currently an Associate Professor with the Computer Engineering Department, King Saud University. His research interests include computer network modeling and simulation, wireless sensor networks, cooperative relay networks, fault tolerance, 5G heterogeneous networks, and high-speed networks.